A Framework for Measuring TRE at the Tip of an Optically Tracked Pointing Stylus

Amber L. Simpson[a], Neal P. Dillon[b], Michael I. Miga[a], Burton Ma[c]

[a] Department of Biomedical Engineering, Vanderbilt University, Nashville, Tennessee, USA
[b] Department of Mechanical Engineering, Vanderbilt University, Nashville, Tennessee, USA
[c] Department of Electrical Engineering and Computer Science, York University, Toronto, Canada

ABSTRACT

We describe a framework for measuring TRE at the tip of an optically tracked pointing stylus. Our approach relied on a robotic manipulator equipped with a spherical wrist to collect large amounts of tracking data from well defined paths. Fitting the tracking data to planes, circles, and spheres allowed us to derive estimates of FLE and precisely localize target locations. A preliminary analysis of our data suggested that there was bias in the registered pointer tip location that depended on the tilt angle of the coordinate reference frame with respect to the tracking system.

1. PURPOSE

The purpose of our work is to develop a framework for empirically determining the precision of an optical tracking system in terms of fiducial localization error (FLE) and target registration error (TRE)[1] so that theoretical models of the behavior of TRE[2–7] can be validated or refuted. In this report, we are primarily interested in describing the framework, reporting on the consistency of the measurements, and reporting the results of measuring TRE as a function of the angle between a tracked coordinate reference frame (CRF) and the viewing direction of the tracking system.

Our approach is designed to measure FLE of markers on a CRF and TRE at the tip of a tracked and calibrated pointing stylus; TRE models have previously been used to model such errors.[7,8] FLE is present in the tracking system measurements of the CRF attached to the pointing device, which induces a TRE at the tip of the pointing device when the calibrated tip location is transformed into the tracking system coordinate frame. If FLE is anisotropic with the largest component oriented along the viewing direction of the tracking system, then the predicted RMS TRE decreases as the CRF is tilted towards and away from the tracking cameras;[7] this is contrary to most users' expectations, and one empirical study of TRE suggest that TRE at the tip of a pointer is smallest when "the largest possible surface area of the pointer's reflecting ball is directed toward the camera".[9]

2. METHODS

We require an estimate of the tracking system FLE covariance and the ability to precisely measure the location of a target in the tracking system coordinate frame. Our approach uses a 6 degrees-of-freedom (DOF) robotic arm where the last three joints are arranged in a spherical wrist configuration and a CRF is attached to the tool flange of the wrist. A spherical wrist is composed of three mutually orthogonal revolute joints whose axes of motion intersect at a point called the wrist center; actuating any combination of the joints produces zero translation of the wrist center which makes the wrist center an ideal target point. Actuating the first joint of the wrist causes the markers of the CRF to move in parallel planes with each marker following a circular path. Actuating the second joint of wrist changes the tilt of the CRF; systematically actuating the first and second joints of the wrist allows us to move the markers of the CRF in parallel circular paths all arranged on the spherical surfaces sharing a common center point located at the wrist center (see Figure 1). Systematically actuating the second and third joints of the arm allows us to change the location of the wrist center while keeping the orientation of the arm parallel to the viewing direction (z axis) of the tracking system. This experimental setup allows us to perform spherical calibrations of a virtual stylus where the CRF is the reference frame attached to the stylus and the wrist center is the tip of the stylus.

Our apparatus consisted of an optical tracking system (Polaris Spectra, Northern Digital Inc., Waterloo, ON, Canada), a planar 4 passive marker CRF (Polaris rigid body part number 8700339, Northern Digital Inc., Waterloo, ON, Canada), a robotic arm (Mitsubishi RV-3S, Mitsubishi Electric and Electronics USA, Inc., Cyprus, CA, USA), and a custom made

Medical Imaging 2013: Image-Guided Procedures, Robotic Interventions, and Modeling,
edited by David R. Holmes III, Ziv R. Yaniv, Proc. of SPIE Vol. 8671, 867114
 doi: 10.1117/12.2008507

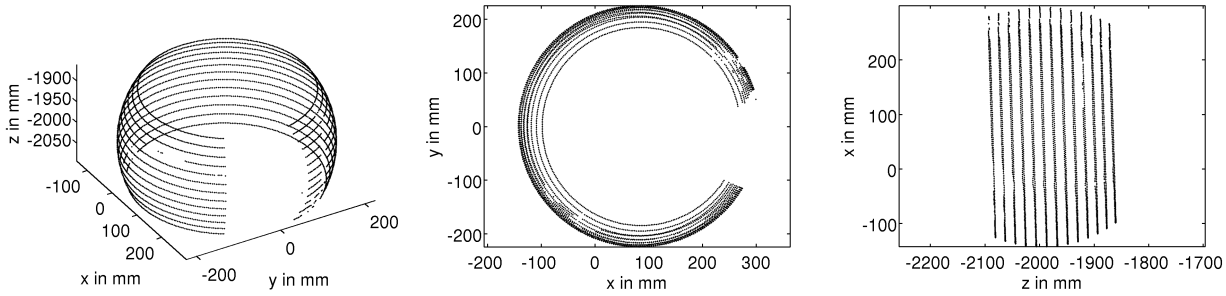

(a) (b) (c)

Figure 1. (a) Raw marker locations in the tracking system coordinate frame for a single marker at a single wrist center location. Small gaps in the circular paths are caused by the tracking system reporting non-visibility of the CRF. The large gap reflects the physical limits of rotation of the first wrist joint. (b) Raw marker locations as viewed along the z axis of the tracking system showing the circular paths travelled by the marker. (c) Raw marker locations as viewed along the y axis of the tracking system showing the planes of the circular paths. Each plane corresponds to a different tilt angle of the CRF with respect to the tracking system; the middle plane corresponds to a tilt angle of 0°.

(a) (b)

Figure 2. (a) The mounting bracket used to fixate the CRF to the flange of the robot. (b) An illustration of the CRF relative to the wrist center of the robot. The wrist center served as the tip of our tracked tool.

mount to attach the CRF to the tool flange of the robot (Figure 2(a)). The mount was designed so that the length of the virtual stylus was approximately 200 mm, the length of a standard tracked tool (Figure 2(b)). The retroreflective spheres on the CRF were new and previously unused. The tracking system was positioned relative to the robotic arm such that the CRF was always in the pyramid volume of the tracking system and the planes of circular motion were as close as possible to perpendicular to the tracking system z axis (i.e., ideally the circles would lie in planes parallel to the xy plane of the tracking system) (Figure 3). The robot joints are illustrated in Figure 4(a). We used 10 different wrist center locations, achieved by systematically moving joints J2 and J3 (Figure 4(b)). At each wrist center location, we collected the CRF raw marker locations on paths spanning -160°–$+160^\circ$* of a circle in 1° increments, at 13 tilt angles spanning -30°–$+30^\circ$ in 5° increments where a tilt of 0° corresponds to the plane of CRF being perpendicular to the tracking system z axis (i.e., the CRF was directly facing the tracking system) (Figure 4(c)). Each measurement was performed with the robotic arm stationary for a period of 1 second.

For every circular marker path, we found the plane of the path using orthogonal regression; because we could not manually inspect the large number of data points for outliers, the regression was computed using statistically robust principal components analysis.[10,11] Each plane was defined by a point on the plane $\mathbf{p}_i$ and a normal vector $\mathbf{n}_i$. The average normal vector $\bar{\mathbf{n}}$ over all of the fitted planes was taken to be the estimate of the true normal vector for all of the circular paths. The

*The range of the physical limits of the first joint of the wrist of this particular robot.

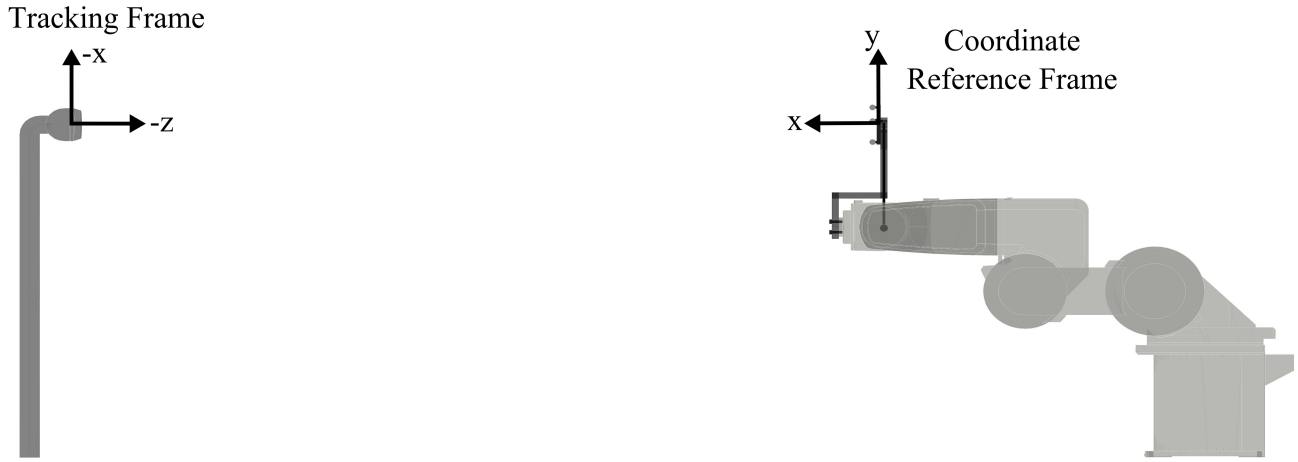

Figure 3. Position of the robotic arm relative to the optical tracking system. The z axis of the optical tracking system was approximately parallel to the robotic arm.

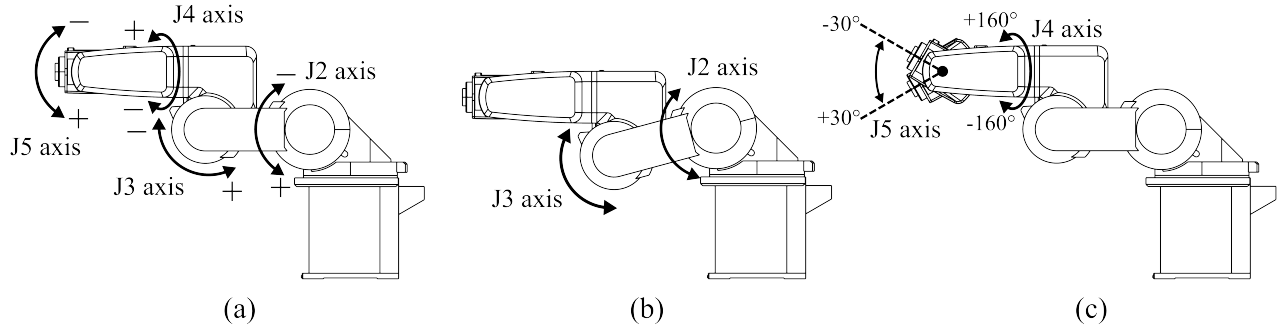

Figure 4. (a) Illustration of the robot joints actuated in the experiment (joint J1 and J6 (not shown) were fixed throughout data collection). (b) Systematic movement of the J2 and J3 joints moved the wrist center of the robot. Ten wrist centers were collected in this experiment. (c) Movement of the J4 joint from -160°–$+160^{\circ}$ produced points on a circular path and movement of the J5 joint from -30°–$+30^{\circ}$ tilted the CRF toward and away from the camera.

rotation $\mathbf{R}$ that aligned $\bar{\mathbf{n}}$ with the z axis of the tracking system was computed.[†] The measured marker locations for each circular path translated by $-\mathbf{p}_i$ and rotated by $\mathbf{R}$ so that they were centered on xy plane of the tracking system. The marker locations were projected onto the xy plane and the best fit circle to each path was found using a Levenberg-Marquardt geometric circle fit (orthogonal regression).[12] The residual errors of the circle fit (measured as the orthogonal distance to the circle in the xy plane) and the plane fit (measured as the distance in the z direction) were computed and covariance of the errors taken to be the estimate of the tracking system FLE covariance $\mathbf{\Sigma}_{\text{FLE}}$.

At each wrist center location, $\mathbf{c}_j$, four spheres were fit to the measured marker locations (one sphere for each of the four markers on the CRF) using an errors-in-variables regression[13] where the error covariance of each marker location was taken to be $\mathbf{\Sigma}_{\text{FLE}}$. The average center location of the four spheres, $\bar{\mathbf{c}}_j$, was taken to be the estimate of the true tip location of the virtual stylus in tracking system coordinates. To find the stylus tip location relative to the CRF, we registered each measurement of the CRF markers to a model of the CRF to find a registration transformation $\mathbf{T}_{k,j}$. The registration transformation was applied to the estimated tip location; averaging over all n_j measurements of the CRF yielded the stylus tip location $\bar{\mathbf{r}}_j = (1/n_j)\sum_{k=1}^{n_j} \mathbf{T}_{k,j}\bar{\mathbf{c}}_j$. The final stylus tip location relative to the CRF, $\bar{\mathbf{r}}$, was taken to be the average location taken over all 10 wrist center locations (i.e., $\bar{\mathbf{r}} = (1/10)\sum_{j=1}^{10} \bar{\mathbf{r}}_j$.) The registration transformations need to be computed using an algorithm that can account for the the anisotropy in $\mathbf{\Sigma}_{\text{FLE}}$; we used the HEIV algorithm.[7,13]

The squared magnitude of TRE for the k^{th} CRF measurement at wrist center location $\mathbf{c}_j$ is simply $\text{TRE}^2_{k,j} = \|\mathbf{T}_{k,j}\bar{\mathbf{c}}_j - \bar{\mathbf{r}}\|^2$. Note that the theoretical models of TRE predict the mean squared magnitude of TRE so the appropriate averaging over multiple TRE^2 values must be performed before comparing empirical and predicted TRE values.

3. RESULTS

Before presenting the FLE and TRE results, we present results confirming that the tracking data was consistent with the expected motion of the robot. First, we confirmed that the circular paths all occurred in parallel planes. There were a total of 520 circular paths (4 markers $\times$ 13 tilt angles $\times$ 10 wrist center locations); the standard deviation in the angle between the fitted plane normal and the average normal direction was 0.02° with a maximum difference of 0.12°.

Second, we confirmed that the radius of the circle travelled by each marker at a given tilt angle was consistent over all wrist center locations. The standard deviation of the fitted circle radii was 0.01 mm with a maximum difference in the estimated radius of 0.13 mm.

Third, we confirmed that the paths travelled by each marker was in fact circular. This could be determined by looking at the standard deviations of the in-plane residual errors after circle fitting. Over all of the paths taken by all of the markers the standard deviations of the fitting errors were 0.02 mm in both the x and y directions of the tracking system.

Fourth, we confirmed that the radius of the sphere travelled by each marker was the consistent over all wrist center locations. The standard deviations of the estimated radii were all less than 0.01 mm with a maximum difference in the estimated radii of 0.02 mm.

Fifth, we confirmed that the centers of the estimated spheres for each marker was consistent at each wrist center location. The standard deviations of the estimated sphere centers was 0.01 mm in the x and y directions, and 0.07 mm in the z direction. We observed that one of the markers produced estimated sphere centers that were consistently biased by approximately -0.12 mm in the z direction compared to the other three markers.

Given the results reported above, we were satisfied that the tracking data was consistent with the expected motion of the robot. Using the residual errors of the circle and plane fits over all 520 circular paths, the FLE covariance was found to be $\mathbf{\Sigma}_{\text{FLE}} = \begin{bmatrix} 0.0004 & -0.0000 & 0.0014 \\ -0.0000 & 0.0003 & -0.0008 \\ 0.0014 & -0.0008 & 0.0369 \end{bmatrix}$; the square root of the sum of the eigenvalues of this covariance matrix is 0.19 mm. This is somewhat smaller than the manufacturers stated accuracy of 0.25 mm RMS; however, the stated accuracy is over the entire pyramid volume whereas our measurements were primarily from the central portion of the pyramid volume.

[†] $\mathbf{R}$ was very nearly the identity matrix because we attempted to align the robotic arm parallel to the viewing direction of the tracking system.

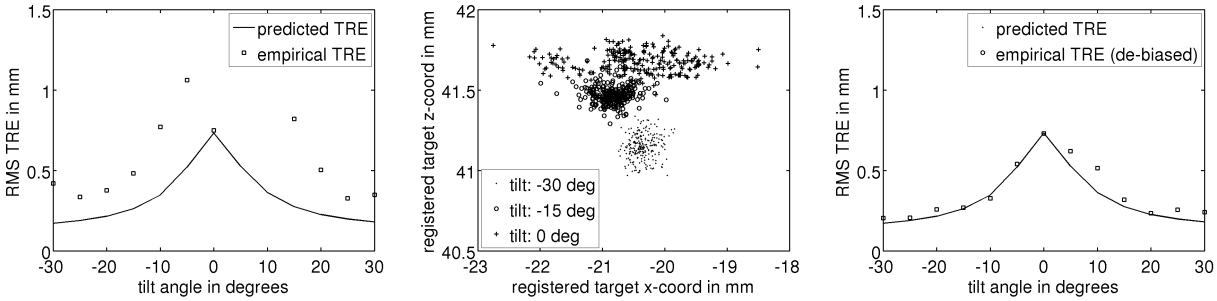

(a) (b) (c)

Figure 5. (a) Empirical versus predicted RMS TRE as a function of CRF tilt angle. (b) Registered target xz locations illustrating obvious clustering by tilt angle. The y component is not shown because the variation is much smaller than in the x and z components. The coordinate frame is the frame of the CRF model. Only three tilt angles are shown for clarity. (c) Empirical versus predicted RMS TRE after de-biasing the registered target locations.

RMS TRE as a function of tilt angle is shown in Figure 5 (a). The empirical TRE was consistently larger than the predicted TRE computed using the spatial stiffness model of TRE.[7] An analysis of the registered target locations (the stylus tip) yielded a surprising observation: the registered target locations were clustered by tilt angle of the CRF (see Figure 5 (b)). It appeared that the tilt angle of the CRF induced a bias in the registered target locations; if the registered target locations are de-biased (by shifting the mean location of each tilt angle cluster to $\bar{\mathbf{r}}$) and the TRE magnitude recomputed we find a better agreement of the predicted and empirical TREs (see Figure 5 (c)).

4. CONCLUSIONS

We have presented a framework for studying FLE and TRE of an optical tracking system. Our preliminary results showed that the straightforward application of theoretical models of TRE magnitude underestimate the magnitude of TRE at the tip of tracked pointing stylus. A closer analysis of our data revealed that there is a bias in the registered target locations that seems to depend on the tilt angle of the CRF relative to the tracking system view direction. De-biasing the registered target locations produced empirical TRE values that more closely agreed with the predicted TRE values.

Our results indicate that more work needs to be done to understand the behavior of TRE. We need to determine if the tilt angle dependent bias is a genuine phenomenon or if it is an artifact of our methods. If the bias is real, then we need to determine why the bias arises so that we might be able to predict and compensate for the bias.

If further testing of our framework proves that our methods are sound, then we can study many other aspects of TRE behavior. For example, we can evaluate the effects of different configurations of markers, different number of markers, different passive marker types (such as the Northern Digital Radix Lens passive marker), active versus passive markers, and motion of the CRF. Other potential topics include validating models of TRE distribution and online prediction of FLE.

5. ACKNOWLEDGEMENTS

This work is funded by the NIH grant R01NS049251 from the National Institute for Neurological Disorders and Stroke and R01CA162477 from the National Cancer Institute. The authors wish to thank Dr. J. Michael Fitzpatrick for his thoughtful advice on data analysis and Dr. Rob Labadie for use of his robotic manipulator.

REFERENCES

[1] Maurer, Jr., C. R., Fitzpatrick, J. M., Wang, M. Y., Galloway, Jr., R. L., Maciunas, R. J., and Allen, G. S., "Registration of head volume images using implantable fiducial markers," *IEEE Transactions on Medical Imaging* **16**(4), 447–462 (1997).

[2] Fitzpatrick, J. M., West, J. B., and Maurer, Jr., C. R., "Predicting error in rigid-body point-based registration," *IEEE Transactions on Medical Imaging* **17**(5), 694–702 (1998).

[3] Fitzpatrick, J. M. and West, J. B., "The distribution of target registration error in rigid–body point–based registration," *IEEE Transactions on Medical Imaging* **20**(9), 917–927 (2001).

[4] Wiles, A. D., Likholyot, A., Frantz, D. D., and Peters, T. M., "A statistical model for point-based target registration error with anisotropic fiducial localizer error," *IEEE Transactions on Medical Imaging* **27**(3), 378–390 (2008).

[5] Sielhorst, T., Bauer, M., Wenisch, O., Klinker, G., and Navab, N., "Online estimation of the target registration error for n-ocular optical tracking systems," in [*Medical Image Computing and Computer-Assisted Intervention (MICCAI 2007)*], Ayache, N., Ourselin, S., and Maeder, A., eds., *Lecture Notes in Computer Science* **2**, 652–659, Springer-Verlag (Oct 2007).

[6] Moghari, M. H. and Abolmaesumi, P., "Distribution of target registration error for anisotropic and inhomogeneous fiducial localization error," *IEEE Transactions on Medical Imaging* **28**(6), 799–813 (2009).

[7] Ma, B., Moghari, M. H., Ellis, R. E., and Abolmaesumi, P., "Estimation of optimal fiducial target registration error in the presence of heteroscedastic noise," *IEEE Transactions on Medical Imaging* **29**(3), 708–723 (2010).

[8] West, J. B. and Maurer Jr., C. R., "Designing optically tracked instruments for image-guided surgery," *IEEE Transactions on Medical Imaging* **23**(5), 533–545 (2004).

[9] Niemann, A., Majdani, O., Lenarz, T., and Leinung, M., "Effects of spatial pointer orientation on the accuracy of intraoperative navigation," in [*81st Annual Meeting of the German Society of Oto-Rhino-Laryngology, Head and Neck Surgery*], (2010).

[10] "LIBRA: A Matlab library for robust analysis." `http://wis.kuleuven.be/stat/robust/LIBRA/` (2012).

[11] Hubert, M., Rousseeuw, P. J., and Vanden Branden, K., "ROBPCA: A new approach to robust principal components analysis," *Technometrics* **47**, 64–79 (2005).

[12] Chernov, N., [*Circular and linear regression: Fitting circles and lines by least squares*], CRC Press (2011).

[13] Matei, B., *Heteroscedastic Errors-in-Variables Models in Computer Vision*, PhD thesis, Rutgers University, New Brunswick, New Jersey (May 2001).